Optimization of Process Parameters for Reentrant Surfaces in Direct Metal Laser Melting

Kathryn Ashby, Zack Fieldman, Pat Kenney, & Todd Rockstroh

GE Aviation, Cincinnati, OH

Abstract

One of the key factors for development and optimization of direct metal laser melting (DMLM) is the analysis of process parameters on reentrant build geometry and surface finish.   Recent studies have focused on the optimization of standard build parameters with only minor emphasis on reentrant geometries. Parameters that are not optimized often contribute to poor surface finish, difficult to remove supports, and failed-to-build geometries of reentrant surfaces that limit the capabilities of DMLM. Through the analysis of multiple studies with varying process parameters and input scan path geometry, open loop methods for creation and control of reentrant build geometries are assessed and presented.

1   Introduction

A recognized hurdle of Direct Metal Laser Melting (DMLM) is the generation of reentrant or downward facing surfaces. (Van Elsen 2007) Reentrant surfaces, at the most extreme condition, occur when attempting to consolidate a layer of powder upon a preceding layer of un-consolidated powder. (Illston 2010) Typical reentrant surface geometries in DMLM include overhanging surfaces, flat surfaces parallel to the build plate, arches, and hollow internal passages as illustrated in Figure 1.   Often times, these surfaces can be generated successfully with the use of base material support structures that may be removed post-build. However, requiring sufficient access to remove said structures precludes the generation of internal passages and features for which the implementation of additive techniques provides the most value.

In the absence of robust support structure, reentrant geometries are oftentimes achievable but with a heightened risk of material and geometry defects. These include linear indications, inconsistent stock loss, degradation of surface finish, and pilling of the outersurface. A further risk is presented by the fact that these surfaces are inherently uninspectable without the use of expensive non-destructive techniques, such as CT scanning, or more expensive destructive evaluation to prove process capability (or lack thereof). These areas of poor part quality lead to limitations on the large-scale production of geometrically conforming parts that meet six sigma process capability standards. The importance of developing reentrant parameters is largely impacted by the need to create a solid base for the structure so that when recoated it is not damaged creating an incomplete first layer. By optimizing parameters for reentrant surfaces the limitations of part geometries and orientations can be overcome eliminating key issues with building unsupported surfaces.   Figure 2 illustrates an example of an overhanging roof that was created in efforts following this trial.

A number of studies have put forth solutions to effectively build reentrant surfaces. These include closed loop controls (Kruth, Mercelis et al. 2007) and in-process build

manipulation(Illston 2010), both of which have drawbacks that may preclude their use in high volume production across a large number of machines and geometries. Techniques for generating reentrant surfaces in other additive modalities have shown promise. (Qi, Singh et al. 2014) Through optimization of the key parameters in DMLM including laser power, scan speed, spot size, and scan spacing, for each material and layer thickness, the best part quality can ultimately by achieved. (Kamath, El-dasher et al. 2014) To reach full density within powder bed additive manufacturing a parameter set that balances each of those key parameters must be created so that material is fully melted without causing keyholing or undersintering the layer. The major hurdle in developing these parameters is the labor intensive trial and error process required to establish the best process window for each material, machine type, and process. To overcome the labor intensity, the goal of this project was to validate a novel method for quick testing parameters within a large range of possibilities while being able to quantitatively evaluate the variation of the machine in a timely and efficient manner.
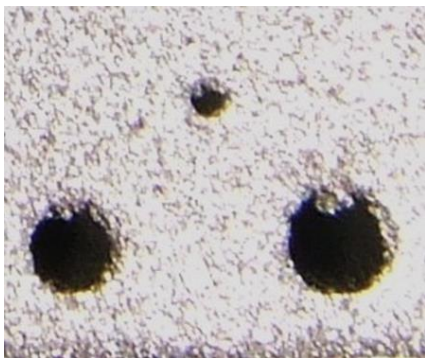

Figure 1: Examples of reentrant surfaces.

Figure 2: Single layer reentrant surfaces.

2   Experimental Procedure

2.1 Overview

To simulate formation of reentrant surfaces into unsintered powder, trials were completed by single exposing unsupported geometries into layers of raw powder. Key output characteristics measured were: mass, thickness, and visual comparison of qualitative material robustness. Across platform variation was identified early on as a risk to output fidelity. (Dadbakhsh, Hao et al. 2012) The first of three stages attempts to mitigate this risk by completing exposures in nine zones across the build platform. The second stage investigated the development of reentrant parameters through the exposure of identical geometries with varying scan speeds and spacings. The final stage compared different process gas flow patterns within the build chamber by looking at variation in different machine models. (Weilhammer 2011)

Experiments were performed using EOS model M270 and M280 DMLM machines with a 200 Watt Fiber laser using Cobalt Chrome alloy powder. For each stage of experimentation, the build platform heating module was disabled to negate the potential effects of thermal heating variation. Process gas and chamber flow behavior was verified

to be steady state throughout the trials while maintaining oxygen content below 1.5% in a Nitrogen atmosphere.

2.2   Platform Variation

The goal of the platform variation study was to investigate variation across the platform in two different flow atmospheres. For the platform variation trial, nine (9) of the 12mm by 12mm samples were laid out in a three (3) by three (3) grid pattern across the build area.   Trials were performed in both the EOS M270 and EOS M280. All parameters were held constant for each sample.

2.3 Parameter Development

For the trials of speed and spacing samples, test specimens were built across the platform in a grid pattern where either speed or spacing increased incrementally in each trial within the ranges outlined in Figure 3.   For each set of experimental parameter conditions, a minimum of two (2) samples was created; sample parameter sets are illustrated in Figure 4. Through this study, several variables that affect these parameters will be investigated including speed, spacing, variation across the build platform, etc. For both speed and spacing samples were single exposed with parameters that vary only that factor from sample to sample. To examine these parameters the Andrews Number, or applied energy density, E_A ,

$$E_A = \frac{P}{U \times SP}$$

where P is the laser power, U is the scan velocity, and SP is the scan or hatch spacing will be applied. (Gibson, Rosen et al. 2010)

Parameter	Range
Laser Power	100-195 Watts
Beam Speed	400-700 mm/s
Hatch Spacing	0.03-0.1 mm
Spot Size	0.070-0.140 mm

Figure 3: Parameters included in the trial and the range tested.

Speed (mm/s)	Spacing (mm)
800	0.03
800	0.05
3200	0.03
3200	0.05
5600	0.03
5600	0.05

Figure 4: Example parameter combinations tested.

3 Discussion of Results

3.1 XY vs. X scanning

Before completing platform variation and parameter development studies, an initial trial was performed to review the differences in macrostructure from scanning using standard processing parameters. These parameters double expose the raw powder in two directions (X & Y). In figure 5, the macrosurface image show a greater surface porosity and thicker rows of metal agglomerates due to the secondary scan this leads to greater stalactite formation when applied to reentrant surfaces of the overall part. The image shows strong indications of overmelt of the material and porosity. Figure 6 shows the single directional scan which has less evidence of over melt and porosity which leads to less surface roughness in the reentrant parameters. By using only single direction scanning on each layer or alternating layer parameter scans better surface finish and decreased porosity is observed.
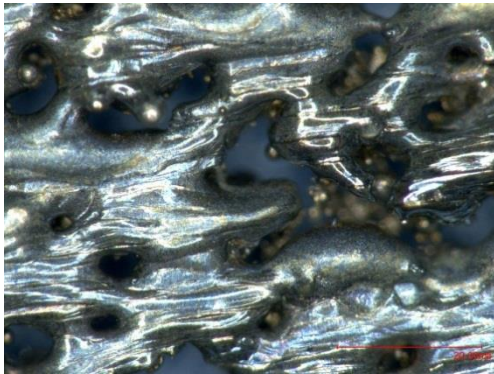

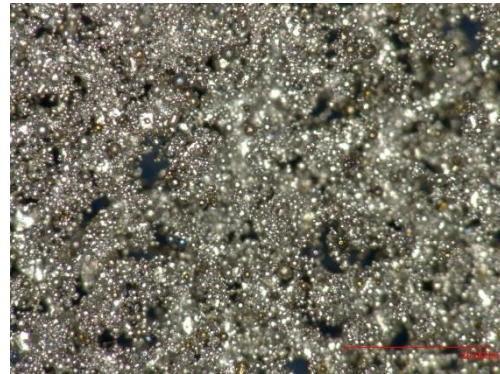**Figure 5: Macrosurface images of samples scanned in X and Y directions.**

Figure 6: Macrosurface images of samples scanned in X direction only.

3.2 Platform Variation

Upon reviewing variation across the platform, two potential hypotheses emerged that could impact the cross platform variation. The first is the role of nitrogen and air flow through the machine due to the placement of the atmosphere intakes and outputs. A potentially more turbulent flow could lead to the poor evacuation of the volatilized powder species within the build chamber. A second is that the variation is due to distortion of the laser as it moves away from the focal point suggesting that specimens in the corners of the build platform would be substantially different than those in the center of the platform. To examine the platform variation, a raw powder burn experiment was conducted in both the EOS M270 and EOS M280. Architecture changes between the M270 and M280 create a more laminar process gas flow scheme across the powder bed. Upon analysis of the mass variation, variability is greater within the M270 machine than in the M280. Figure 7 and figure 8 show variation across the platform from front to back in both machines. However, the range of the data is almost two times greater for the M270 than the M280. Based on this data, there is still evidence of platform variation not caused by

the flow pattern suggesting that other factors like distortions of the laser are affecting the overall variation.
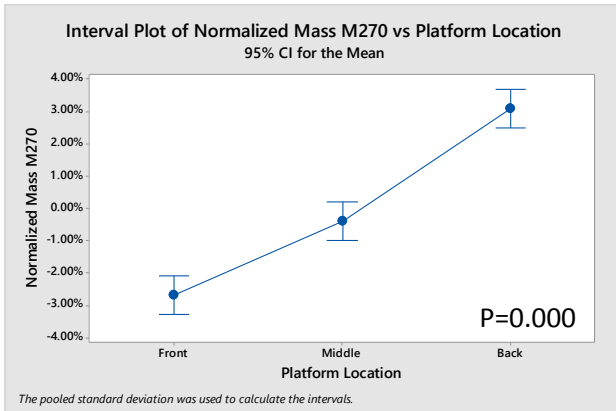

Figure 7: ANOVA comparing platform variation front to back in an M270.
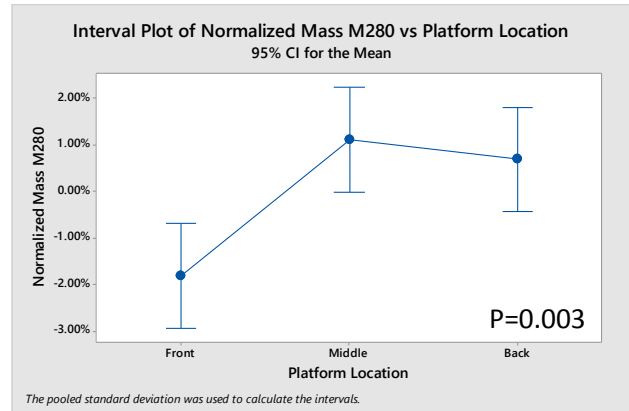

Figure 8: ANOVA comparing platform variation front to back in an M280.

For the left to right platform variation, as shown in figure 9 and 10, both p-values are greater than 0.05 therefore we fail to reject the null hypothesis that there is platform variation front to back. The p-values suggest that platform variation is substantially less for each machine from left to right.
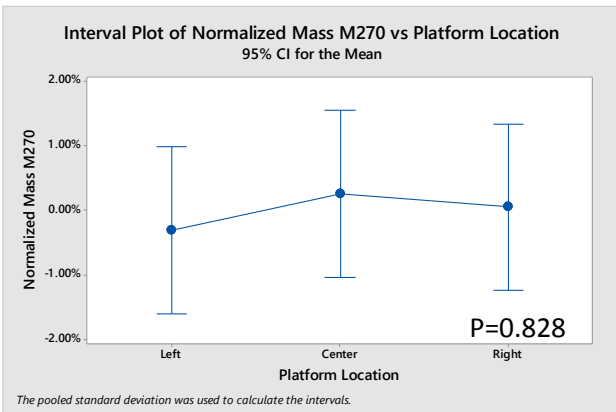

Figure 9: ANOVA comparing platform variation left to right in an M270.
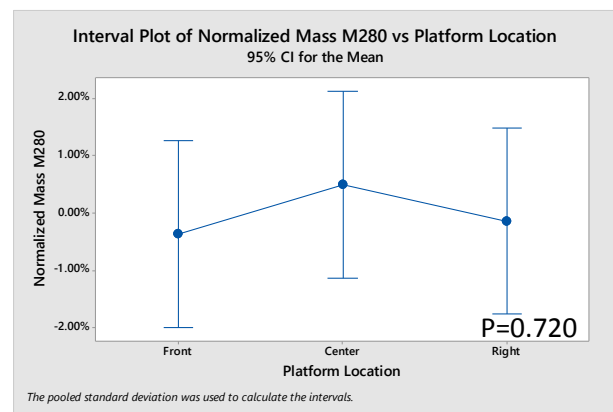

Figure 10: ANOVA comparing platform variation left to right in an M280.

3.3 Parameter Development

Using the Andrews number, mass and thickness were graphed for each spot size. As shown in figures 11 and 12, a spot size of 0.070mm shows a strong correlation between the Andrews number and both mass and thickness. Conversely, a spot size of 0.140 mm, as illustrated in figure 13 and 14, shows a much lower r-squared value and greater variation.
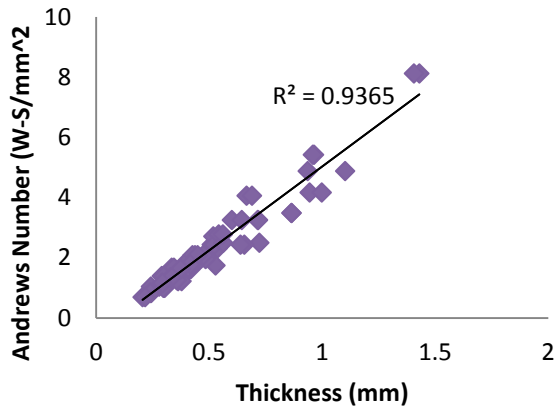
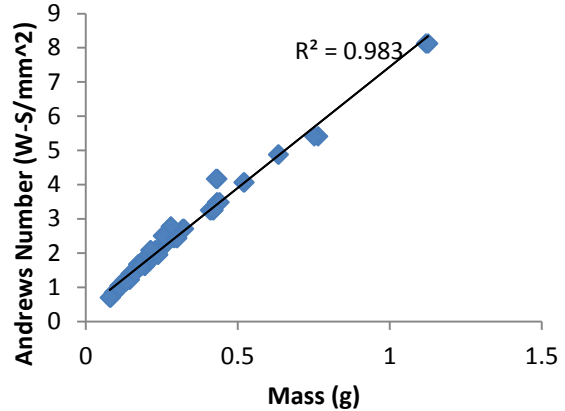**Figure 11: Thickness compared to the Andrews Number at a 0.070 mm spot size.**

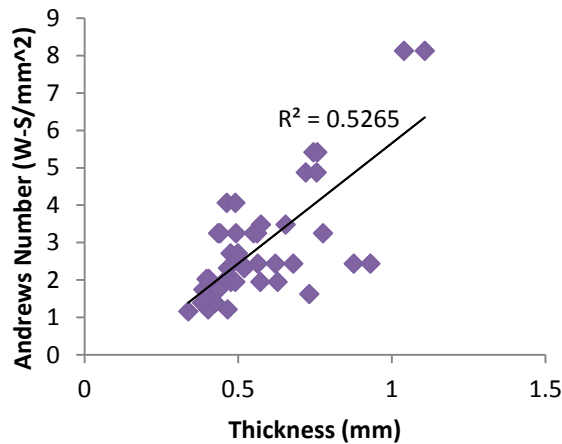**Figure 12: Mass compared to the Andrews Number at a 0.070 mm spot size.**

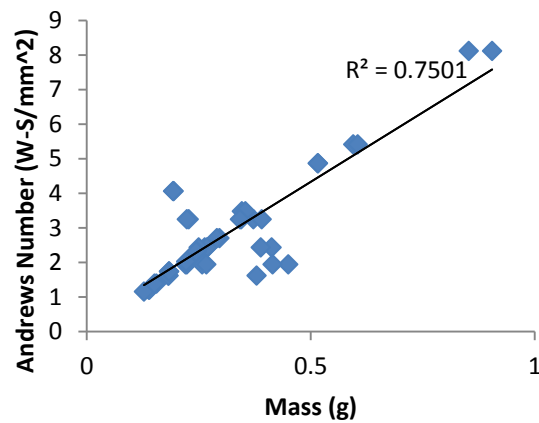**Figure 13: Thickness compared to the Andrews Number at a 0.140 mm spot size.**

Figure 14: Mass compared to the Andrews Number at a 0.140 mm spot size.

The significantly greater variation at the 0.140mm spot size indicates that the variation within the laser is greater at a large spot size. In part, this is due to the bending of the laser as it moves across the platform as well as the physical machine design for spot size adjustment.

Throughout these samples, four unique failure modes were determined: balling, warpage out of the recoat plane, lack of fusion, and poor overmelting as illustrated in figure 14. Within each of these trials, parameters of speed and spacing were varied until each of the failure modes was achieved. It was hypothesized that the optimized reentrant parameter set would be the sample with the greatest density without entering any of the failure modes because it offers the strongest parameter set to be able to withstand the recoater.

Figure 14: Failure modes from left to right: lack of fusion, balling, overmelting, and warpage out of the recoater plane.

From these trials, the parameter set that was observed to have the greatest density without entering one of the failure modes was 5600 mm/s speed, 0.03mm spacing, and 0.070mm spot size.

4   Conclusions

Surface finish quality is a key challenge to the proliferation of additive manufacturing into widespread use. This paper demonstrates a simple approach to improvement of reentrant surfaces, the worst performing surfaces of the additive process. The proposed approach seeks to better understand the contributing factors to poor reentrant surfaces by decoupling the generation of them from the standard bulk material parameters.

Use of a fully focused spot size and laminar process gas flow demonstrate reduced variability in output surface quality. The Andrews number continues to demonstrate usefulness in balancing laser speed versus path spacing tradeoffs. Additional work is required to understand the spot size energy impact to surface finish. Future studies will focus on expanding the understanding of platform variation, integration of reentrant parameters into full part parameters, and implementation of novel part geometries currently unattainable within the laser powder bed additive process.

Bibliography

1. Dadbakhsh, S., L. Hao and N. Sewell (2012). "Effect of selective laser melting layout on the quality of stainless steel parts." <u>Rapid Prototyping Journal</u> 18(3): 241-249.
2. Gibson, I., D. W. Rosen and B. Stucker (2010). <u>Additive manufacturing technologies</u>, Springer.
3. Illston, T. J. (2010). initiate the formation of a re-entrant feature reversibly bonding the unfused underlying powder such that it is stable under the application of laser; able to prevent balling up of the powder, but still be able to reverse the bonding allowing subsequent removal of the powder from the article, Google Patents.
4. Kamath, C., B. El-dasher, G. Gallegos, W. King and A. Sisto (2014). "Density of additively-manufactured, 316L SS parts using laser powder-bed fusion at powers up to 400 W." <u>The International Journal of Advanced Manufacturing Technology</u>: 1-14.
5. Kruth, J.-P., P. Mercelis, J. Van Vaerenbergh and T. Craeghs (2007). <u>Feedback control of selective laser melting</u>. Proceedings of the 3rd international conference on advanced research in virtual and rapid prototyping.
6. Qi, H., P. Singh, D. B. Desander, M. N. Azer, S. K. Tewari, M. D. Gledhill, J. G. Sabato and T. J. Rockstroh (2014). Method for Fabricating Turbine Airfoils and Tip Structures Google Patents.
7. Van Elsen, M. (2007). "Complexity of Selective Laser Melting: a new optimisation approach."
8. Weilhammer, J. (2011). <u>EOSINT M</u>. IUM 2011.